

Geochemistry, Geophysics, Geosystems®



RESEARCH ARTICLE

10.1029/2021GC010268

Key Points:

- Femtosecond-laser ablation inductively coupled plasma mass spectrometry provides a new approach on distinguishing Mn of the ontogenetic shell calcite from Mn of the authigenic coatings
- Ontogenetic Mn within the foraminifer shell calcite may result from the regional nutrient cycle
- Mn in the deep eastern Caribbean Sea may mainly derive from hydrothermal sources along the Antilles Island Arc

Supporting Information:

Supporting Information may be found in the online version of this article.

Correspondence to:

N. Ögretmen,
ogretmenn@itu.edu.tr;
nazikogretmen@gmail.com

Citation:

Ögretmen, N., Schiebel, R., Jochum, K. P., Galer, S., Leitner, J., Khanolkar, S., et al. (2022). High precision femtosecond laser ablation ICP-MS measurement of benthic foraminiferal Mn-incorporation for paleoenvironmental reconstruction: A case study from the Plio-Pleistocene Caribbean Sea. *Geochemistry, Geophysics, Geosystems*, 23, e2021GC010268. <https://doi.org/10.1029/2021GC010268>

Received 17 NOV 2021

Accepted 24 AUG 2022





Author Contributions:

Conceptualization: N. Ögretmen
Data curation: N. Ögretmen, J. Leitner
Formal analysis: N. Ögretmen, J. Leitner, B. Stoll, U. Weis
Investigation: N. Ögretmen
Methodology: N. Ögretmen, K. P. Jochum, S. Galer, J. Leitner, B. Stoll, U. Weis

© 2022. The Authors.

This is an open access article under the terms of the [Creative Commons Attribution-NonCommercial-NoDerivs License](https://creativecommons.org/licenses/by/4.0/), which permits use and distribution in any medium, provided the original work is properly cited, the use is non-commercial and no modifications or adaptations are made.

High Precision Femtosecond Laser Ablation ICP-MS Measurement of Benthic Foraminiferal Mn-Incorporation for Paleoenvironmental Reconstruction: A Case Study From the Plio-Pleistocene Caribbean Sea

N. Ögretmen^{1,2} , R. Schiebel¹ , K. P. Jochum¹, S. Galer¹, J. Leitner¹ , S. Khanolkar^{1,3}, M. Yücel⁴, B. Stoll¹, U. Weis¹ , and G. H. Haug^{1,5}

¹Max Planck Institute for Chemistry, Mainz, Germany, ²Now at Evolution and Ecology Department, Istanbul Technical University, Eurasia Institute of Earth Sciences, Istanbul, Turkey, ³Now at GEOMAR Helmholtz-Zentrum für Ozeanforschung, Kiel, Germany, ⁴Institute of Marine Sciences, Middle East Technical University, Mersin, Turkey, ⁵Department of Earth Sciences, ETH Zürich, Zürich, Switzerland

Abstract Closure of the Central American Seaway (CAS) and hydrology of the Caribbean Sea triggered Northern Hemisphere Glaciation and played an important role in the Pliocene to modern-day climate re-establishing the deep and surface ocean currents. New data on Mn/Ca obtained with femtosecond laser ablation inductively coupled plasma mass spectrometry on well-preserved tests of the epibenthic foraminifer *Cibicidoides wuellerstorfi* and infaunal *C. mundulus* contribute to the interpretation of paleoenvironmental conditions of the Caribbean Sea between 5.2 and 2.2 Ma (million years) across the closure of the CAS. Hydrothermal activity at the Lesser Antilles may be a primary source of Mn in the well-oxygenated Plio-Pleistocene Caribbean Sea. Incorporation of Mn in the benthic foraminifer shell carbonate is assumed to be affected by surface ocean nutrient cycling, and may hence be an indicator of paleoproductivity.

Plain Language Summary The closure of the Panama Isthmus caused the expansion of ice sheets in the Northern Hemisphere and changed the water current dynamics and climate in the Caribbean Sea since the Pliocene (~5.3 million years ago). New Mn/Ca data measured using femtosecond laser ablation inductively coupled plasma mass spectrometry on the deep-sea benthic foraminifer species *Cibicidoides wuellerstorfi* and *Cibicidoides mundulus* help us understand past environmental conditions of the Caribbean Sea prevailed between 5.2 and 2.2 million years ago. While manganese might be sourced from the surrounding hydrothermal vents, its incorporation in the foraminifer shell carbonate might be related to nutrient cycling and may indicate past biological productivity in the ocean.

1. Introduction

Trace elements in foraminiferal calcite are among the most commonly used proxies for reconstructing paleoenvironmental conditions. For instance, Mg/Ca of foraminifer test carbonate is proxy of past temperature variations of ambient seawater (Friedrich et al., 2013; Lear et al., 2000; Nürnberg et al., 1996). B/Ca is used as a surface seawater pH proxy (Yu et al., 2007). In contrast to the proxies of environmental conditions during shell formation, some trace elements are considered proxy of dissolution or encrustation of the original test carbonate. For example, trace metal oxides may crystallize through post-mortem secondary precipitation processes such as authigenic coatings on the foraminifer test (Boyle, 1983) and vigorous cleaning techniques are required for their removal (Barker et al., 2003). Nevertheless, a recent study demonstrates that such cleaning methods cause dissolution of the inner calcite resulting in removal of potentially important environmental indicators including Mn (Fritz-Endres & Fehrenbacher, 2020). Novel results suggest Mn is preferentially incorporated in the ontogenetic carbonate lattice to enhance its chemical stability (Soldati et al., 2016; Son et al., 2019).

In oxygenated waters, manganese is dissolved at low concentration (van Hulst et al., 2017), with a residence time of up to 60 years in the water column below 1,500 m (Martin & Knauer, 1980). In seafloor sediments, Mn is found in oxidized forms only in the uppermost oxic layer, and mobilizes under suboxic and anoxic conditions as Mn(II) as well as Mn(III)-ligand complexes (Trouwborst et al., 2006), being an indicator of

Resources: R. Schiebel, G. H. Haug
Supervision: R. Schiebel
Validation: N. Ögretmen
Visualization: N. Ögretmen
Writing – original draft: N. Ögretmen, R. Schiebel, K. P. Jochum, J. Leitner
Writing – review & editing: N. Ögretmen, R. Schiebel, K. P. Jochum, S. Galer, S. Khanolkar, M. Yücel, G. H. Haug

the oxygenation state of the bottom waters, that is, anoxic or oxic (Calvert & Pedersen, 1993). Manganese is an essential micronutrient in the water-splitting step of photosynthesis as well as in reactive oxygen species detoxification (Browning et al., 2021; Sunda et al., 1983; Wu et al., 2019). Organic matter including phytodetritus is consumed by marine organisms such as foraminifers (Gooday et al., 1990; Thomas & Gooday, 1996), and manganese oxides act as a terminal electron acceptor in organic matter degradation in seafloor sediments.

In neritic environments, the ratio of manganese to calcium (Mn/Ca) relates to the input of terrestrial matter such as dust. For example, Sayani et al. (2021) and Thompson et al. (2015) used coral Mn/Ca values to reconstruct wind patterns in the tropical Pacific correlating with El Niño events. Schöne et al. (2021) suggested that high Mn/Ca in bivalve shells may relate to reduced dissolved oxygen (e.g., hypoxia) while low Mn-incorporation during oxygen-depleted conditions points to diminished dissolved manganese inflow.

In foraminifer shells, Mn/Ca has been considered contamination, and Mn has been regarded as overgrowth/coating on the tests (Barker et al., 2003; Boyle, 1983). Nonetheless, foraminiferal Mn/Ca has been used to interpret oxygenation states of past ocean waters (Chen et al., 2017; Ni Fhlaithearta et al., 2018) and terrestrial matter input (Klinkhammer et al., 2009). Munsel et al. (2010) point out that hydrothermal vents or pollution in seawater may result in trace metal enrichment in the foraminiferal shell. Davis et al. (2020) relate the foraminiferal Mn/Ca to deep-water upwelling. Another study suggests Mn-incorporation into the planktic foraminifer shell by volcanogenic input from the Toba super-eruption (Lemelle et al., 2020).

With the new advanced techniques in paleoclimate and paleoceanography, it is possible to gather more information on previously studied sites that had crucial impacts on past ocean-climate dynamics, such as the Caribbean Sea. The Caribbean Sea is situated in a key location (Figure 1a) for the configuration of paleo- and modern-climate settings and triggering climate extremes such as the glaciations of the Quaternary (De Schepper et al., 2013; Haug & Tiedemann, 1998; Haug et al., 2001).

In the present study, we focus on the use of manganese and evaluate its potential as paleo-proxy attempting to explore the reasons for exceptionally high benthic foraminiferal Mn/Ca in the well-studied Caribbean Sea accounting for volcanic activity, riverine input, microbial processes, and photosynthesis. We present Mn/Ca values of benthic foraminifer tests and contribute to interpretations on paleoenvironmental conditions of the Caribbean Sea between 5.2 and 2.2 Ma across the closure of the Central American Seaway (CAS). The incorporation of Mn and other metals such as Na, Mg, and Sr in deep-sea benthic foraminiferal tests, as well as $\delta^{18}\text{O}$ and $\delta^{13}\text{C}$, are being discussed as proxies of environmental conditions during the Plio-Pleistocene. Our results facilitate a better understanding of foraminifer Mn-incorporation and its relationship to the remineralization processes of organic matter.

2. Geology of the Caribbean Region and Its Present-Day Hydrological Setting

2.1. Geological Setting

The collision between the Central American Peninsula and South America as the Pacific Farallon Plate subducted beneath the Caribbean and South American plates at around 73 Ma and triggered the early uplift of the northern Andes (O’Dea et al., 2016). The convergent plate tectonics led to the shoaling of the Panama region starting at ca. 13 Ma until 2.7 Ma when the surface water exchange ceased completely (Haug et al., 2001; Kirillova et al., 2019; Newkirk & Martin, 2009).

The island arc of the Greater and Lesser Antilles as a gateway of the NADW inflow into the Caribbean Basin is shaped by strike-slip fault tectonics with differential vertical movements (Calais et al., 2016). The inflow of the AAIW into the Caribbean Basin has been affected by the development of the Lesser Antilles Volcanic Arc (LAVA) since the late Cenozoic, as a response to the subduction of the American Plate under the Caribbean Plate (Bouysse & Westercamp, 1990). The subduction process has been bearing new volcanic islands along the Lesser Antilles including St. Vincent in the south and Montserrat in the north (Bouysse & Westercamp, 1990; Jackson, 2013) while shaping the bathymetry with the emergence on the eastern exterior fore-arc (Münch et al., 2014) and submergence on the inner western back-arc due to extensional tectonics (Allen et al., 2019).

Consequently, the inter-island passages in between these newly formed volcanic islands (Figures 1a and 1b), where the deep waters enter the Caribbean Basin, have been directly affected by the formation of the island arcs.

2.2. Present-Day Hydrography

The ODP Site 999A is located in the Colombian Basin in the western Caribbean Sea. The surface waters of the Caribbean Sea consist of a mixture of South Atlantic waters from the Guyana Current and Equatorial waters from the North Equatorial Current (Figure 1a). The deep waters are composed of a mixture of nutrient-depleted high- $\delta^{13}\text{C}$ (ventilated) NADW below 1,000 m water depth, and corrosive nutrient-enriched low- $\delta^{13}\text{C}$ (oxygen-poor) AAIW between ~ 500 and 1,000 m water depth (Gröger et al., 2003), experiencing only limited renewal as the younger colder waters sink to the deeper water column (Sturges, 1970). The NADW enters the Caribbean from the north through the passages of the Greater and Lesser Antilles, whereas the AAIW enters from the southwest through the passages of Lesser Antilles (Figures 1a and 1b; Schmuker & Schiel, 2002, and references therein).

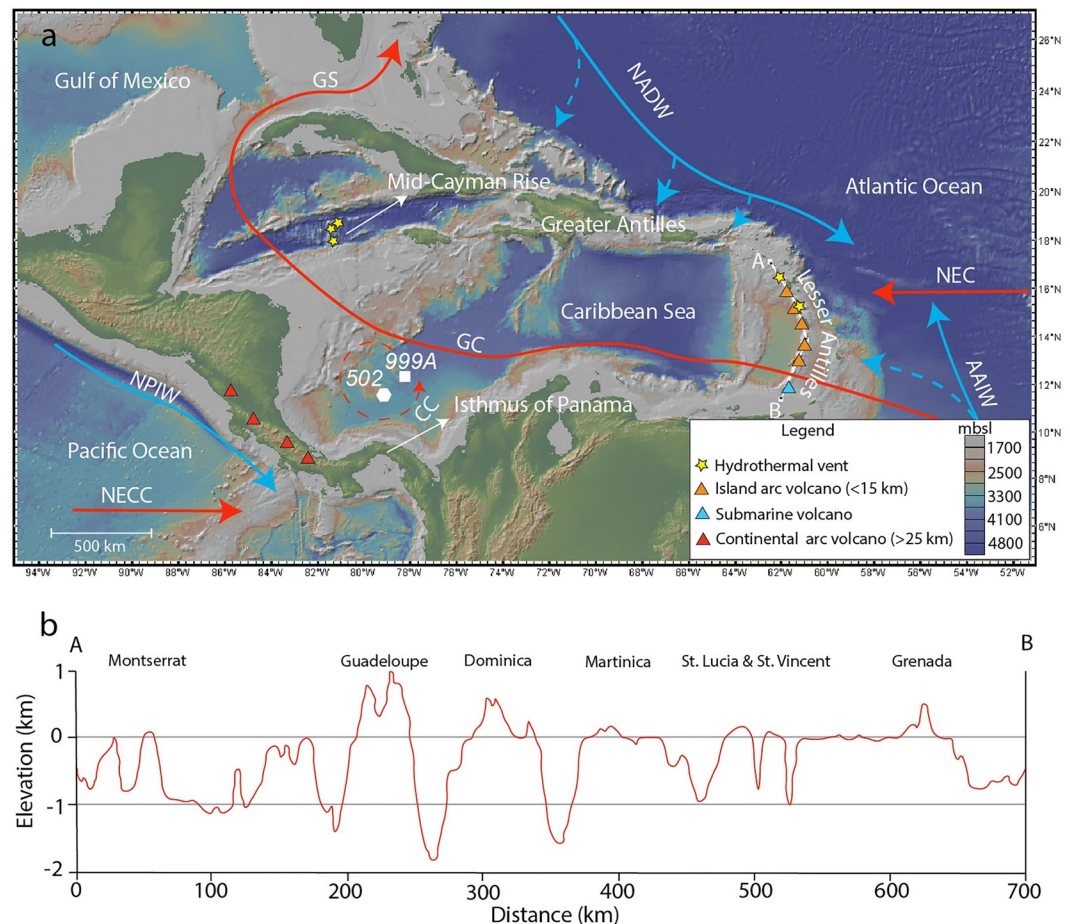


Figure 1. (a) Simplified map showing active volcanoes, hydrothermal vents, and hydrographic setting of the circum-Caribbean Sea (after Öğretmen et al., 2020a and references therein; GS: Gulf Stream; GC: Guyana Current; CC: Caribbean Current; NEC: North Equatorial Current; NADW: North Atlantic Deep Water; AAIW: Antarctic Intermediate Water; NPIW: North Pacific Intermediate Water; NECC: North Equatorial Counter Current). ODP Site 999A and DSDP Site 502 are shown in white square and hexagon, respectively. Active volcanoes and hydrothermal vents are marked with triangles and stars, respectively, and detailed in legend. (b) Section from A to B (a) demonstrates the elevation of the Lesser Antilles islands and the depth-width of main water exchange passages. The base map (a) and section (b) produced using GeoMapApp. Data on volcanic activity were obtained from the Smithsonian Global Volcanism Program List and hydrothermal vent data were obtained from InterRidge Vent Database v2.1 (Beaulieu et al., 2013).

3. Material and Methods

3.1. Femtosecond LA-ICP-MS Trace Element Analyses

ODP Site 999A was drilled during Leg 165 in the Caribbean Sea, Colombian Basin, at 12°44.639'N, 78°44.360'W, at 2,827.9 m water depth (Shipboard Scientific Party, 1997).

Well-preserved glassy specimens of the benthic foraminifers *Cibicidoides wuellerstorfi* and *Cibicidoides mundulus* were picked from the >250 μm size fraction and cleaned in the clean laboratory at the Max Planck Institute for Chemistry (MPIC) applying oxidative cleaning (Barker et al., 2003). Criteria for visual identification of preservation state were adapted from Schneider et al. (2017) and Sexton et al. (2006) based on shell surface preservation, reflectance, transparency, and color. Femtosecond laser ablation inductively coupled plasma mass spectrometry (LA-ICP-MS) analyses were carried out on 142 specimens of *C. wuellerstorfi* and 87 specimens of *C. mundulus* covering the period from 5.2 to 2.2 Ma for *C. wuellerstorfi* and 5.2–3.2 Ma for *C. mundulus*. To investigate the paleoenvironmental conditions including oxygen concentration in ambient seawater, we measured Mn/Ca in the shells of *C. wuellerstorfi* and *C. mundulus* at high-resolution on up to the last five chambers of each specimen (Figures 2 and 3a). After applying oxidative cleaning, specimens were placed on a sandbath (pure >250 μm-sized quartz grains) to avoid any possible contamination during femtosecond laser ablation inductively coupled plasma mass spectrometry (fs-LA-ICP-MS).

Trace element analyses ($^{55}\text{Mn}^+$ and $^{43}\text{Ca}^+$ for *C. wuellerstorfi*; ^{23}Na , ^{88}Sr , ^{55}Mn , ^{25}Mg , and ^{43}Ca for *C. mundulus*) were conducted on single specimens applying fs-LA-ICP-MS method in the Paleoclimate Laser Laboratory at the MPIC. Mn-coatings and lattice-bound Mn-incorporation were analyzed from $^{55}\text{Mn}^+ / ^{44}\text{Ca}^{++}$ laser ablation profiles of the same specimens as used for trace element analyses (Figure 2). Laser ablation profiles were acquired

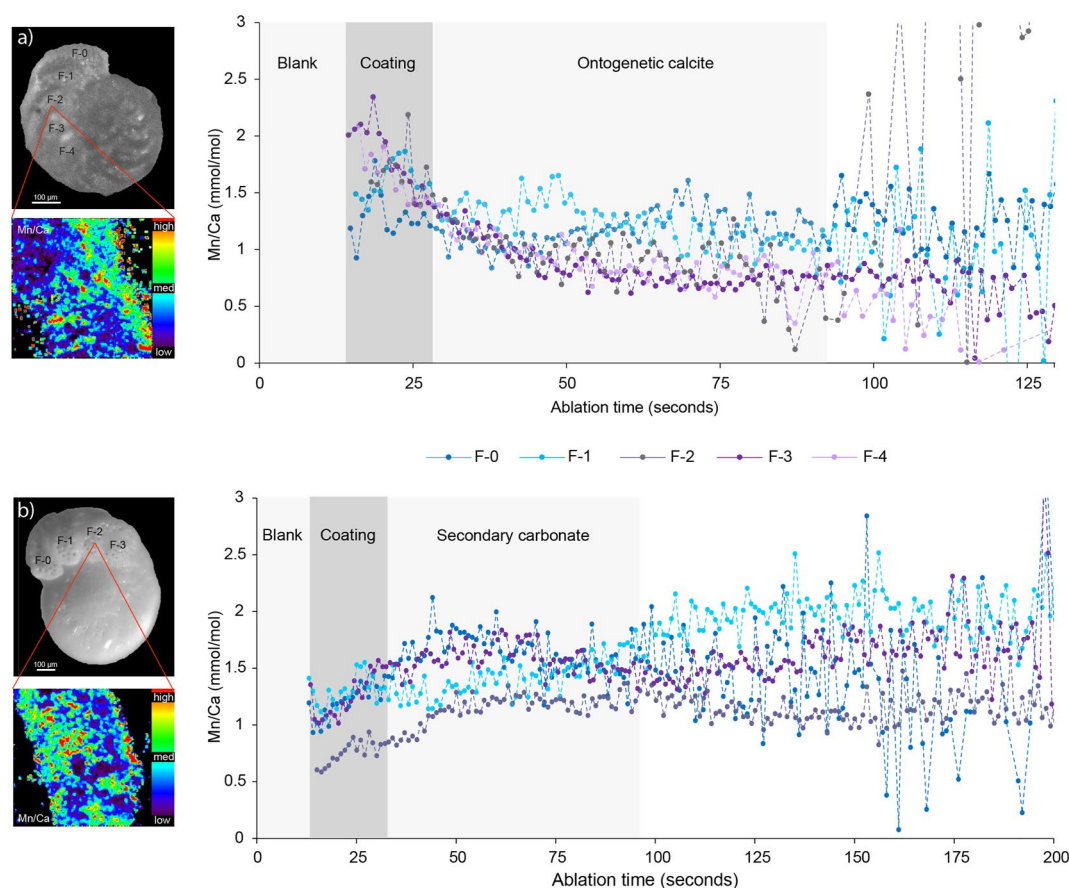


Figure 2. Gray-scale light microscope images (scale bars 100 μm), NanoSIMS Mn/Ca maps (25 × 25 μm), and fs-LA-ICP-MS profiles on Mn/Ca of well (a) and poorly (b) preserved specimens of *C. wuellerstorfi*. Mn/Ca scales are the same for both (a) well and (b) poorly preserved tests.

on 30- μm diameter spots per chamber with a pulse repetition rate of 1 Hz. Trace element analyses were performed on a 25- μm diameter spot on each chamber with a pulse repetition rate of 15 Hz at low fluence (0.1–0.3 J/cm²). To avoid possible polyatomic interferences that might result in similar elemental mass as ⁵⁵Mn (e.g., ³⁹K¹⁶O), tuning was applied to minimize oxide formation (ThO/Th <0.3%). Calibration was performed with the microanalytical carbonate reference material USGS-MACS-3 (Jochum et al., 2019). Important operating parameters are given in Supporting Information S1 (Table S1).

For trace element measurements and laser ablation depth profiles, data reduction was applied using Excel routines as described by Jochum et al. (2007) for trace elements, and Jochum et al. (2019) for single-shot laser ablation depth profiles. Excel routine data reduction permits identification of electronically induced outliers that might deviate from the average of ~40 measured values derived during the single-shot trace element measurement. A correction factor is computed from the MACS-3 carbonate reference material to calibrate all measured Mn/Ca values throughout the measurement for single-shot laser ablation depth profiles.

For paleoenvironmental interpretation, we compared our data with data from DSDP Site 502 on infaunal/epifaunal foraminifer data and flux of organic carbon values provided by Jain et al. (2007) (Figure 3a). Stable isotope values were adopted from Haug and Tiedemann (1998) and Haug et al. (2001). Alkenone-based pCO₂ data are from Seki et al. (2010). Other trace element values (Na, Mg, and Sr) of *C. wuellerstorfi* were adopted from Ögretmen et al. (2020b) and plotted against the new *C. mundulus* trace element data (Figures 3d–3f). Our measurements with fs-LA-ICP-MS yield reproducible results with a relative standard error between 2% and 6%.

3.2. Nanoscale-Secondary Ion Mass Spectrometry (NanoSIMS)

After oxidative cleaning, well-preserved, and, for comparison of the preservation state, poorly-preserved specimens of *C. wuellerstorfi* from different core depths were embedded with epoxy resin, ground, and polished to obtain a smooth surface of equatorial sections for trace element analysis with nanoscale-secondary ion mass spectrometry (NanoSIMS).

Secondary ion images of ⁵⁵Mn⁺ and ⁴⁰Ca⁺ from selected sample areas were acquired in multi-collection mode with the NanoSIMS 50 ion probe at the MPIC (Hoppe et al., 2013). Prior to analysis, fields slightly larger than the intended measurement areas were cleaned with a high current primary beam (~40 pA) to remove the gold coating on selected sample areas. With the recently installed Hyperion RF plasma oxygen primary ion source, a primary O⁻ beam (d ~250 nm, 15 pA) was scanned over 22 × 22 μm^2 - to 28 × 28 μm^2 -sized sample areas. Three to four image planes (256 × 256 pixels) were acquired, with integration times of 10 ms/pixel each. From the ion data, ⁵⁵Mn/⁴⁰Ca⁺ maps were generated, using software developed at the MPIC.

3.3. Principal Components Analysis

Principal Components Analysis (PCA) was applied to the benthic foraminifer trace element/Ca matrix on the new Mn data set, combined with previous Mg, Sr, Na (Ögretmen et al., 2020b), and $\delta^{13}\text{C}$ and $\delta^{18}\text{O}$ (Haug et al., 2001; Haug & Tiedemann, 1998) data using the PAST software version 4.03 (Hammer et al., 2001). The PCA is used to quantify relationships within the multivariate data set (Hammer et al., 2001). Bootstrapping was carried out with 999 bootstrap replicates for all analyses, to estimate the variance of factor loadings (Chatterjee, 1984). In the scree plots, 95% bootstrapped confidence intervals are given for each Eigenvalue, and the broken stick values are reported (see Figures S1, S2, and S3 in Supporting Information S1). For all analyses, the first two components lie above the broken stick values. Therefore, these two components have been considered for further interpretation (Table S1 in Supporting Information S1). The loadings given in Table S2 in Supporting Information S1 reveal to what degree the original variables describe the different components. Principal Component loadings >0.3 were considered for further interpretation.

4. Results

4.1. Trace Element Analyses

To investigate the distribution of Mn in the crystal lattice, fs-LA-ICP-MS depth profiles of well and poorly preserved specimens of *C. wuellerstorfi* and 2D-NanoSIMS maps of *C. wuellerstorfi* were obtained (Figures 2a

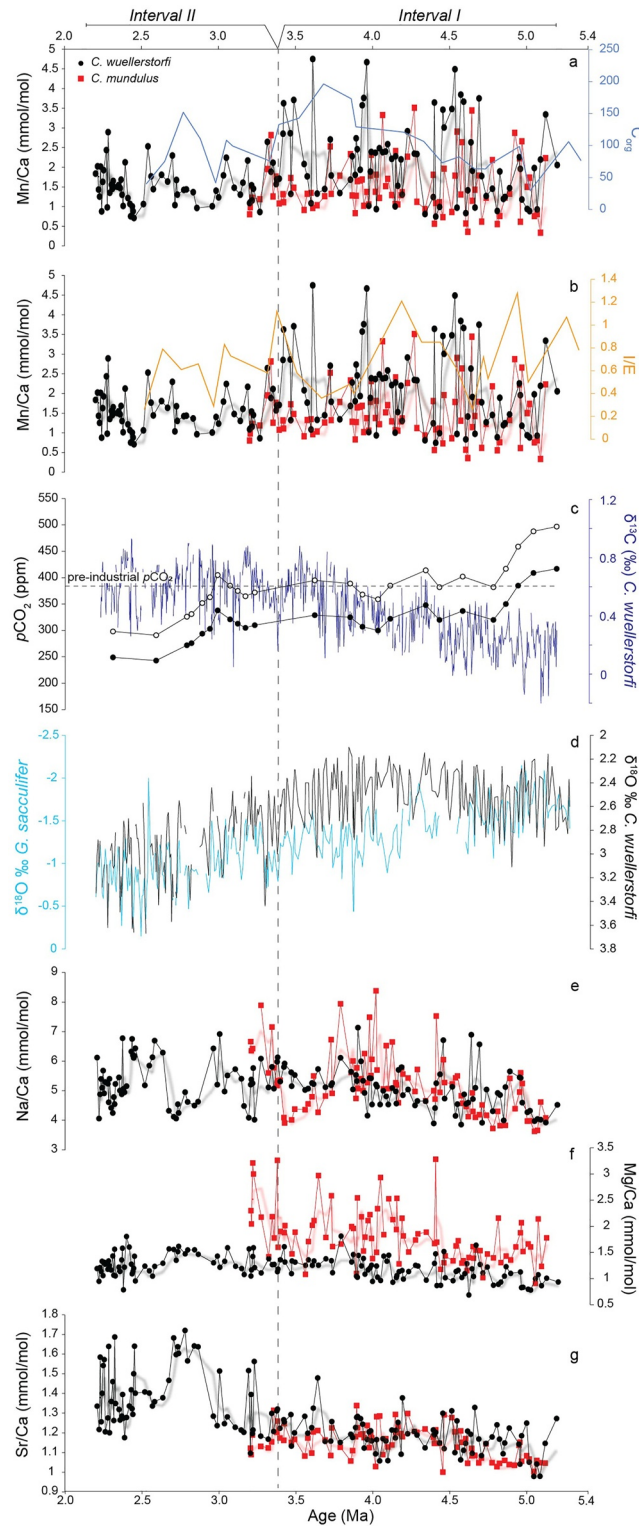


Figure 3. Trace element values of *C. wuellerstorfi* and *C. mundulus* cover the time interval from 5.2 to 2.2 Ma and 5.1 to 3.2 Ma, respectively. Mn/Ca of *C. wuellerstorfi* and *C. mundulus* together with (a) C_{org} (flux of organic carbon to the seafloor, C_{org}) as an indicator of paleoproductivity and (b) Infaunal/Epifaunal (I/E) data as an indicator of oxygenation (Jain et al., 2007). (c) Alkenone-derived maximum and minimum pCO_2 for atmospheric CO_2 as a driver of warming (Seki et al., 2010) and $\delta^{13}C$ as an indicator of deep-water ventilation (Haug & Tiedemann, 1998). (d) $\delta^{18}O$ values of both planktic and benthic foraminifers (Haug & Tiedemann, 1998; Haug et al., 2001) as indicators of ice volume changes and paleotemperature. (e) Na/Ca of *C. wuellerstorfi* and *C. mundulus* as a potential indicator of paleosalinity. (f) Mg/Ca of *C. wuellerstorfi* and *C. mundulus* as an indicator of paleotemperature. (g) Sr/Ca values of *C. wuellerstorfi* and *C. mundulus* as an indicator of terrestrial input. The Na/Ca, Mg/Ca and Sr/Ca data of *C. wuellerstorfi* are adopted from Ögretmen et al. (2020b).

and 2b). Even well-preserved specimens are characterized by high Mn/Ca coatings and lower values in the ontogenetic test wall (Figure 2a). The coating may be of authigenic origin. In contrast, poorly-preserved specimens show lower Mn/Ca in the outer layer and higher Mn/Ca through the test wall of the foraminifers (Figure 2b). Laser ablation times may vary from specimen to specimen depending on the test thickness and density, the latter of which may be affected by preservation state of the calcite lattice (Figure 2). Mn/Ca maps from NanoSIMS analyses show the heterogeneous distribution of Mn within the shell wall of *C. wuellerstorfi* with higher Mn/Ca near the shell surface of some tests (Figure 2a). In contrast, Mn/Ca in poorly-preserved tests is rather patchy with higher Mn/Ca at the inner layers of the shell wall (Figure 2b). The alteration of tests has been described as minor, moderate, and major (Ni et al., 2020). However, specimens analyzed in our study (Figure 2b) do not show any signs of moderate or major alteration such as invisible pores or irregular overgrowths on the outer surface described by Ni et al. (2020). We did not analyze pore geometry, which was shown of unsuitable criterium for test preservation state by Torres et al. (2010). Instead, we have followed the optical criteria of Schneider et al. (2017) and Sexton et al. (2006) to assess the preservation state of the specimens analyzed here.

4.1.1. Trace Metal/Ca of *C. wuellerstorfi*

Between 5.2 and 3.3 Ma, Mn/Ca varies at high values up to 4.5–4.7 mmol/mol with an average of ~ 2.1 mmol/mol (Figure 3a). The same time interval is marked by slightly increasing Na/Ca from ~ 3.9 mmol/mol to up to 7.1 mmol/mol with a mean of ~ 5.0 mmol/mol. While high Mn/Ca are observed between 5.2 and 3.3 Ma, a decreasing trend between 3.6 and 3.3 Ma leads to a significant change from 4.7 mmol/mol to values as low as 0.7 mmol/mol with an average of 1.5 mmol/mol after 3.3 Ma until 2.2 Ma. Mn/Ca values significantly (*t*-test) drop from the time-interval of 5.2 and 3.3 Ma to 3.3- and 2.2 Ma ($p < 0.05$). Consequently, we distinguish two intervals, *Interval I* (5.2–3.3 Ma), and *Interval II* (3.3–2.2 Ma). Across the 3.3 Ma time-level between *Interval I* to *II*, no significant change in Na/Ca is observed, and significant mid-term variation in Na/Ca occurs only after 3.3 Ma (Figure 3d).

4.1.2. Trace Metal/Ca of *C. mundulus*

Throughout the time interval (5.2–3.2 Ma), Mn/Ca of *C. mundulus* varies less than in *C. wuellerstorfi* and ranges at lower values between maximum ~ 3.5 mmol/mol and minimum ~ 0.4 mmol/mol (Figure 3a). Na/Ca shows an increasing trend from 5.2 Ma until ~ 3.8 Ma, from 3.6 mmol/mol up to 7.9 mmol/mol, and a sharp minimum as low as 4 mmol/mol at 3.4 Ma before rising to > 7 mmol/mol at 3.3 Ma (Figure 3d). Sr/Ca show an increasing trend from 5.2 to 3.3 Ma, and little variation at 1–1.3 mmol/mol (Figure 3e). In comparison to *C. wuellerstorfi*, Mg/Ca of *C. mundulus* are more variable between 0.36 mmol/mol and 3.5 mmol/mol (Figure 3e).

4.2. Environmental Indicators of the Plio-Pleistocene Caribbean Sea

PCA was applied to trace element values of Na/Ca, Mg/Ca, Mn/Ca, Sr/Ca, and stable isotope values $\delta^{13}\text{C}$ and $\delta^{18}\text{O}$ of *C. wuellerstorfi* for (a) the complete time interval (5.2–2.2 Ma), (b) the time interval between 5.2 and 3.3 Ma (*Interval I*), and (c) the time interval between 3.3 and 2.2 Ma (*Interval II*) following the Mn/Ca development over time (Figure 3a). Only data from the epibenthic *C. wuellerstorfi* are included in the PCA, as it lives and represents the bottom water conditions other than the infaunal *C. mundulus*. The results of the PCA reveal two relationships that prevailed in the Pliocene Caribbean Sea and show varying dominance throughout both *Intervals I* and *II*. For *Interval I*, Principal Component (PC) 1 is positively correlated with Mn/Ca, and PC two is positively correlated with Na/Ca. In contrast, in *Interval II*, PC 1 is represented by Na/Ca, and PC two positively correlates with Mn/Ca (see Supporting Information S1).

5. Discussion

5.1. Ontogenetic Incorporation of Mn in the Foraminifer Shell Carbonate

Close to the oxygen minimum layer in the sediment, the aragonitic shells of the shallow infaunal benthic foraminifer *Hoeglundina elegans* show an increase in Mn-incorporation (Reichert et al., 2003). A similar increase

occurs at high manganese concentration in the sedimentary pore fluids (Reichert et al., 2003). Even though it has been documented that the symmetrical octahedral crystal structure of calcite can accommodate Mn^{2+} easier than the asymmetric aragonite structure (Soldati et al., 2016), the high concentration of dissolved manganese in suboxic ambient waters might have potentially facilitated the incorporation of Mn in aragonitic *H. elegans* shell, serving as a micronutrient to the live organism (Browning et al., 2021; Wong et al., 2022). Alternative to a sedimentary Mn source, Mn may be derived from a suboxic water column, reaching the benthic habitat as marine snow (Alldredge & Cohen, 1987). Both potential Mn sources the surface sediment or bottom water column may facilitate foraminiferal Mn-incorporation in different environmental settings, and explain differences in the Mn/Ca of the well and poorly preserved test carbonate (Figures 2a and 2b, respectively).

5.2. Diagenetic Incorporation of Mn in the Foraminifer Shell Carbonate

Diagenesis refers to post-depositional physical and chemical changes of the original seafloor sediment including foraminifer tests. On the deep sea floor, it occurs close to the sediment-water interface where the pore fluids may cause reprecipitation of carbonate (Boyle, 1983; Froelich et al., 1979). Therefore, it is a process that alters the carbonate mineralogy enabling redox-sensitive elements to take place in the carbonate mineral structure substituting calcium in the crystal lattice (Johnson et al., 2016). In dissolution-precipitation processes, it has been suggested that calcium preferentially remains in the liquid phase during abiotic carbonate precipitation (Pangitore, 1978). Given its smaller cation radius compared to calcium (Pangitore, 1978), manganese may replace calcium producing relatively higher Mn/Ca values (Figure 2b). Diagenesis can occur as neomorphism resulting in the replacement of primary biogenic calcite with abiotic calcite ending up with an opaque instead of glassy appearance (Figure 2b, see Supporting Information S1; Poirier et al., 2021). Diagenetic processes may include overgrowths on the test (Boyle, 1983) or filling of pores and chamber volumes with finer sediments (Kozdon et al., 2013; Pearson & Burgess, 2008; Sexton et al., 2006). Manganese-rich mineral overgrowths are generally attributed to available Mn^{2+} in suboxic/anoxic sediment pore fluids (Boyle, 1983). Reduced manganese in the pore waters may diffuse upward in the sediment stack (Froelich et al., 1979) and eventually oxidize to precipitate as Mn-overgrowths/Mn-oxides on the sediment surface and foraminifer tests (Boyle, 1983; Calvert & Pedersen, 1993). Such enrichment of Mn-oxides on the sediment surface of the Arabian Sea with oxic deep waters was shown by Schenau et al. (2004) and linked to organic matter flux, which induces Mn^{4+} reduction and results in upward diffusion to the oxic sediment-water interface. As elevated Mn-oxide concentration is not reported from the ODP Site 999A (Sigurdsson et al., 1997), an alternative scenario is discussed for high foraminiferal Mn/Ca values in the Plio-Pleistocene Caribbean Sea in the following chapter.

5.3. Trace Elements as Environmental Indicators

Between *C. wuellerstorfi* and *C. mundulus*, we observe a significant difference in Mn/Ca values from 5.2 to 3.2 Ma (Figures 3a and 3b), which may result from different microhabitat preferences of infaunal *C. mundulus* in comparison to epifaunal *C. wuellerstorfi* (Jorissen et al., 2007; Rathburn & Corliss, 1994). As Mn is a redox-sensitive element, higher and oscillating Mn/Ca of epibenthic *C. wuellerstorfi* may represent the oxygen content of the deep-water column overlying the seafloor sediment, whereas the more constant and lower Mn/Ca of *C. mundulus* may result from an infaunal habitat and less oxygenated interstitial pore waters leading to less Mn-oxide formation. The influence of habitat preference is reflected also by Mg/Ca concentrations. In contrast to *C. wuellerstorfi*, *C. mundulus* is characterized by highly fluctuating values attributable to interstitial pore waters (Figure 3g). This comparison confirms the reliability of epifaunal *C. wuellerstorfi* for paleothermometry studies (Kozdon et al., 2013). As SEM photos of the specimens used in this study do not show any significant diagenesis imprints (Figure 2; see Supporting Information S1), we assume the data set derived in this study is reliable for environmental evaluation. Since *C. wuellerstorfi* is available throughout the studied age interval, we do not use the trace element results of *C. mundulus* for further interpretation.

Our results show that Mn/Ca values of *C. wuellerstorfi* in the time *Interval I*, from 5.2 Ma until 3.3 Ma strongly vary from 0.9 mmol/mol up to 4.7 mmol/mol, but show a constant increase (Figure 3a). A similar increase is notable in Na/Ca values (Figures 3a and 3e; Ögretmen et al., 2020a). The PCA for *Interval I* confirms this trend, with high factor loadings of Mn/Ca in PC 1 and Na/Ca in PC 2 (Tables S2 and S3 in Supporting

Information S1). Our results are in agreement with previous findings, which suggest an oxic environment based on oxygen sensitivity of the benthic foraminiferal assemblages and low infaunal/epifaunal (I/E) benthic foraminifer values throughout the complete time interval (Figure 3b), whereas C_{org} increases from 5.2 Ma until ~3.6 Ma and declines thereafter (Figure 3a; Jain et al., 2007). The increase we observe in Mn/Ca from 5.2 Ma until 3.6 Ma, and the decrease in Mn/Ca during *Interval II* (Figures 3a and 3b) are parallel to the variation in organic carbon flux (Figure 3a; Jain et al., 2007). Slightly increasing ambient bottom water temperatures are inferred from Mg/Ca values of *C. wuellerstorfi* for the same time interval (Figure 3f). However, PCA results indicate that variations in NADW inflow across the closure of the CAS influenced Na/Ca values more than Mg/Ca values (see Supporting Information S1), confirming previous findings (Haug & Tiedemann, 1998; Ögretmen et al., 2020a).

Manganese in foraminifer tests, in general, is attributed to reducing conditions in the interstitial pore water within the sediment resulting in secondary precipitation of Mn-oxides as coatings on the outside of tests as mentioned above (Boyle, 1983). If this was the case, elevated foraminifer Mn/Ca may have related to the warming of ocean waters and an increasing Mn solubility (Ardelan & Steinnes, 2010). At the same time, warming would have increased the stratification of the surface water column. Increasing SSTs would have led to the deepening of the thermocline, and the decrease of the oxygen content of the deeper water bodies (Shepherd et al., 2017). Even though warming of the surface waters of the Caribbean Sea and decreasing planktic foraminifer $\delta^{18}O$ are well documented over the time interval from 5.2 Ma to 3.3 Ma resulting from the closure of CAS (Figure 3d; Steph et al., 2006, 2010; Haug et al., 2001) there is no evidence of prevailing reductive conditions in the bottom water column and surface sediment. On the contrary, well-oxygenated conditions and an increase in epifaunal species in benthic assemblages were reported by Jain et al. (2007), as well as increasing benthic foraminifer $\delta^{13}C$ (Figures 3a–3c; Haug & Tiedemann, 1998). Furthermore, pCO_2 did not show any significant variation throughout the Pliocene until the onset of the Northern Hemisphere Glaciation (Seki et al., 2010), and hence does not point to any increase in reducing conditions in bottom waters affecting Mn/Ca variation across the time *Intervals I* and *II* (Figure 3c).

On the other hand, decreasing paleoproductivity in the Caribbean Sea following 3.6 Ma (Figure 3a; Jain et al., 2007) may have hindered the transport of Mn^{2+} down the water column. In ocean surface waters, Mn is used as a micronutrient by the autotrophs and associated with organic matter produced by phytoplankton, which is exported to the seafloor and remineralized in the benthic realm (Browning et al., 2021).

During the remineralization of organic matter in the presence of oxygen, the components of organic matter are broken down into inorganic forms by microbial activity through respiration (Bianchi et al., 2018). In oxic waters, during nitrification, ammonium (NH_4^+) can be oxidized to nitrate (NO_3^-) via nitrite (NO_2^-), and nitrogen (N_2) can be directly generated in the presence of oxidants such as particulate MnO_2 , which, in return, may produce dissolved Mn^{2+} (Figure S4 in Supporting Information S1; Luther III et al., 1997; Schoemann et al., 1998). Alternatively, Allredge and Cohen (1987), Bianchi et al. (2018), and Shanks and Reeder (1993) suggest that in oxygenated ambient waters denitrification can occur within reducing microhabitats in settling particles such as marine snow where microzones of nutrient enrichment take place and NO_3^- is reduced to N_2 through microbial respiration (Figure S4 in Supporting Information S1). Both processes may result in the dispersal of Mn^{2+} in ambient waters once Mn is decomposed from the degraded organic matter through nitrification and/or denitrification. Whichever of these processes may prevail, the Mn^{2+} would be preferentially incorporated in the calcareous foraminifer shell and increase its chemical stability (Soldati et al., 2016; Son et al., 2019).

Hypothesizing that ontogenetic foraminifer Mn/Ca is affected by one of these two biological processes, varying C_{org} , a product of organic matter degradation, should be parallel to the Mn/Ca of the foraminifer shell (Figure 3b; Jain et al., 2007). This phenomenon is the most plausible explanation for the high Mn/Ca in the foraminifer test calcite and seems to have played an important role in the variation of foraminiferal Mn/Ca values through *Intervals I* and *II* as before and after 3.3 Ma, respectively (Figure 3a). Haug and Tiedemann (1998) and Haug et al. (2001) located the start of the closure at ~3.25 Ma, which seems to be parallel to C_{org} and Mn/Ca variation though the influence of the complete closure at 2.7 Ma is not reflected on C_{org} and Mn/Ca values (Figure 3b). This finding brings forward the necessity of an additional scenario to the CAS closure, which governs the benthic microhabitat. Even if benthic foraminiferal Na/Ca reflects the salinity changes and Mg/Ca points to the temperature variation in the bottom waters (Figure 3e; Ögretmen et al., 2020b) across the CAS closure in four

time-intervals, these do not seem to play an important role in the ecological setting of the benthic fauna as Mn/Ca values and C_{org} reveal different time-slices.

To summarize, our results lead us to consider that Mn plays a role in the local and regional nutrient cycle, and seems to affect denitrification and nitrification processes, resulting in Mn-incorporation in the foraminifer shell calcite. Therefore, further studies accompanying our findings will pave the way for the understanding of Mn/Ca as a proxy of the paleonutrient cycle.

5.4. Source of Mn in the Caribbean Sea

As Mn may be received from terrestrial sources (Klinkhammer et al., 2009), it may correlate with the distribution of strontium (Sr). In the eastern Caribbean, Sr/Ca is related to the increased riverine input from the Magdalena River corresponding to the uplifting Andes across the CAS closure (Ögretmen et al., 2020b). However, Mn/Ca and Sr/Ca do not show any statistically significant relationship ($r^2 = 0.07$, $p < 0.05$; see the PCA results in Supporting Information S1). Contrasting to Sr/Ca increase, Mn/Ca values decrease after ~ 3.5 Ma (Figure 3a), suggesting foraminifer Sr/Ca and Mn/Ca are controlled by different mechanisms that work in different directions, and only 7% of the variability may result from similar processes such as terrigenous/atmospheric input (see Supporting Information S1).

While the source of Mn in the Caribbean waters is not well-constrained, emerging evidence from seafloor hydrothermal vents indicates that high concentrations of dissolved-Mn(II) and Mn(III) in ocean waters and Mn-oxide deposits are mainly related to hydrothermal activities (Middag, de Baar, Laan, & Klunder, 2011). Mn(II) in hydrothermal plumes may have longer oxidation half-lives than much of the other trace metals (e.g., iron, copper, zinc) dispersing over a distance of more than 4,000 km from the vent (Gartman & Findlay, 2020; Resing et al., 2015; Yücel et al., 2021). Being surrounded by the Lesser Antilles Volcanic Arc (LAVA) in the east, and the Central American Volcanic Arc (CAVA) in the west, the Caribbean Sea may receive Mn from volcanic sources (Homoky et al., 2011) and hydrothermal inputs (Frank et al., 2006) (Figure 1a). Whereas the activity of the continental CAVA system was not associated with metalliferous materials ceased from 6.5 Ma until < 2 Ma (Wegner et al., 2011), the LAVA is an island arc system (Jackson, 2013) with a mafic composition (Halbach et al., 2002), that is, associated with metalliferous sediments and fluids being enriched in Mn (Cronan & Johnson, 2001). Dissolved manganese typically ranges around 0.2 nM/kg in open ocean settings (Schlitzer et al., 2018) and 3.2 nM/kg in regions of volcanic activity (Middag, de Baar, Laan, Cai, et al., 2011). High Mn-incorporation in benthic foraminifers such as *Elphidium batialis* is reported, for example, from the Bering Sea in the Aleutian Arc (Detlef et al., 2020).

Donnelly (1973) evidenced the continuous volcanic activity in the LAVA from the Pliocene until today, with diminished activity during the mid-Pliocene (~ 3.6 – 3.5 Ma). The top part of the last volcanoclastic sediment unit deposited in the Guadeloupe archipelago (Figure 1b) dates from the late Piacenzian-early Gelasian at ~ 3 – 2.5 Ma (Münch et al., 2014). Osborne et al. (2014) analyzed foraminiferal coatings for Pb isotopes from the ODP Site 999A across the closure of the CAS, which are assumed to derive from the same volcanic sources as the Mn, and are analyzed from the same foraminiferal coatings obtained from the ODP Site 999A (Figure 4; Osborne et al., 2014). Interestingly, foraminiferal $^{207}\text{Pb}/^{204}\text{Pb}$ and $^{206}\text{Pb}/^{204}\text{Pb}$ values show similarities to volcanic rocks of Montserrat and Dominica (Figure 4; Lindsay et al., 2005; Thirlwall et al., 1996) compared to other volcanic rocks in the region (Cassidy et al., 2012; Labanieh et al., 2010), which might be the source of Pb isotopes and Mn preserved in the foraminiferal coating. The Pb isotope fingerprint matches well with the increasing Mn/Ca values until ~ 3.6 and decreasing Mn/Ca afterwards, suggesting that surrounding volcanism might have supplied Mn to the Caribbean waters. However, during *Interval II* post- 3.3 Ma (Figure 3a), Mn/Ca ranges below the confidence level (PCA, see Supporting Information S1) suggesting ceasing Mn supply from the LAVA. Pb-isotope values from the Fe-Mn crust may identify the WNADW (Abouchami et al., 1999) and North Atlantic (von Blanckenburg et al., 1996) as additional Mn sources to the eastern Caribbean Sea, whereas the Saharan dust input (Kumar et al., 2018) seems to be irrelevant (Figure 4).

Today, there are several active submarine hydrothermal volcanoes and vents in the circum-Caribbean region, such as Kick'em Jenny in the vicinity of Grenada, and Beebe at the Mid-Cayman Rise (Figure 1a). However, the chemical compositions of these vents are not particularly enriched in Mn (Koschinsky et al., 2007; Webber et al., 2014), and we can merely speculate about any submarine volcanic Mn sources in the Pliocene in the same

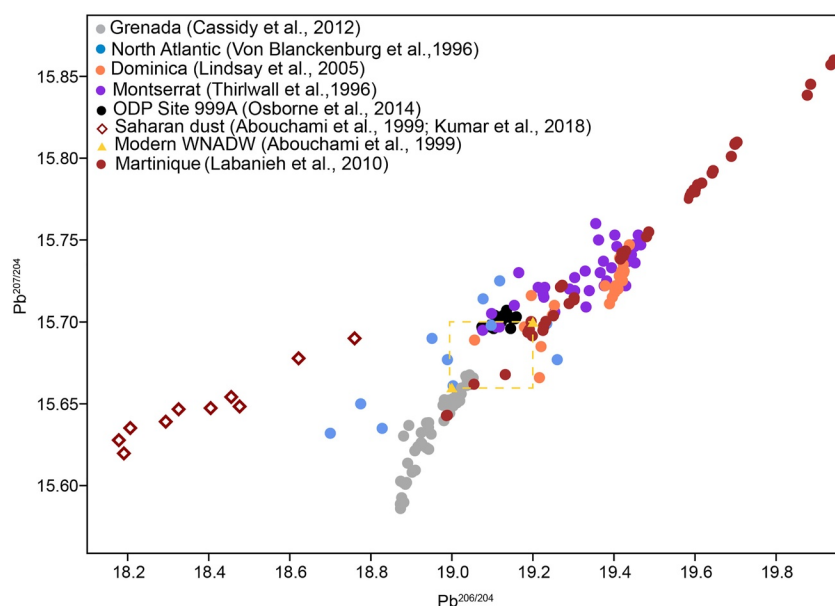


Figure 4. Pb-isotope data from surrounding volcanic rocks in the circum-Caribbean Region (Cassidy et al., 2012; Labanieh et al., 2010; Lindsay et al., 2005; Thirlwall et al., 1996), North Atlantic (von Blanckenburg et al., 1996), from foraminifer coatings (ODP Site 999A; Osborne et al., 2014), and modern values from the Saharan dust (Kumar et al., 2018) and WNADW (Abouchami et al., 1999). Yellow dashed rectangle refers to the Pb-isotope range from the WNADW according to Abouchami et al. (1999).

region. Nonetheless, for example, Montserrat and Dominica islands host active hydrothermal vents (Figures 1a and 1b) and are enriched in Mn (Halbach et al., 2002) dispersed in the deep Caribbean Sea by the inflowing waters through the Lesser Antilles passages. Moreover, McGee et al. (2021) reported high Mn values within the enclaves of Montserrat volcanic rocks, with signatures of an injection of mafic magmas rich in volatiles, which may have contributed to trace metal transported to the sampling Site 999A. Both Mn sources near Montserrat and Dominica may have been active during the Pliocene given the volcanic arc evolution of the Lesser Antilles throughout the Cenozoic.

5.5. Role of Vertical Movements of the Lesser Antilles Passages as Surface and Deep Water Gateway

In the following, we discuss the potential role of tectonics in the Lesser Antilles region in regulating the paleoenvironmental conditions during the Plio-Pleistocene. Paleocirculation of the Plio-Pleistocene Caribbean Sea has been investigated mainly for the shoaling of the Isthmus of Panama (e.g., Haug & Tiedemann, 1998), suggesting that the eastern Caribbean did not experience great vertical variations in bathymetry/topography since the Oligocene-Miocene (Driscoll & Diebold, 1999).

Today, the Lesser Antilles host several Pliocene carbonate platforms on the eastern side of the island arc, and volcanoes along the western side (Bouysse & Westercamp, 1990; Robertson, 2009), which separated as a result of a change in the inclination of the subducting slab during the late Neogene (Burke, 1988). The carbonate platforms show differential uplift rates of some 50–300 m (Bouysse & Westercamp, 1990) controlled by the regional tectonics (Münch et al., 2014), and would result in shoaling of the sill depths of the Lesser Antilles passages eventually reducing the inflow of the AAIW and the NEC into the Caribbean Sea (Figures 1a and 1b). This small-scale shoaling would sufficiently reduce the dispersal of the volcanic materials from the Lesser Antilles as the AAIW and NEC inflow would be reduced. The Pliocene uplift and consequent small-scale shoaling of the Lesser Antilles passages possibly correspond to lowered Mn/Ca after 3.3 Ma (Figure 3a). However, neither the tectonic/volcanic nor biogeochemical (nutrient concentrations and C_{org} flux) alone may explain the variations of Mn/Ca values, which may be considered to result from a complex interplay of Mn sources, and processes that affect Mn incorporation in the foraminifer shell under oxic conditions.

6. Conclusion

Femtosecond LA-ICP-MS provides a new approach on the role of manganese in deep water benthic ecology, distinguishing Mn of the ontogenetic shell carbonate from Mn of the authigenic coatings. Our data indicate that Mn within the ontogenetic foraminifer shell carbonate may be related to, and derived from the regional nutrient cycle, and benthic foraminifer Mn/Ca may be used as an indicator of ocean paleoproductivity. In contrast, the coatings on top of the foraminifer shells are assumed authigenic and affected by the oxygenation state of the bottom waters. The Mn in the deep eastern Caribbean Sea may be mainly derived from hydrothermal sources along the Antilles Island Arc, as well as riverine or atmospheric input from the surrounding continents. Varying Mn concentrations in the regional water bodies are discussed to result from varying NADW and AABW inflow into the Caribbean since the Pliocene. Our results confirm previous studies, which have documented variations in organic carbon flux to the seafloor across the CAS closure between 5.2 and 2.2 Ma.

Our results bring forward the limitations that need to be addressed in future studies to better understand the biogeochemistry of deep marine benthic realms. For example, modern-day measurements of dissolved manganese and biological productivity together with other biogeochemical proxies (e.g., nitrogen isotopes) may enhance our systematic understanding of proxies and paleoclimate.

Conflict of Interest

The authors declare no conflicts of interest relevant to this study.

Data Availability Statement

The data set is available at Mendeley Data <https://doi.org/10.17632/bps7nw7922.1>.

References

- Abouchami, W., Galer, S. J. G., & Koschinsky, A. (1999). Pb and Nd isotopes in NE Atlantic Fe–Mn crusts: Proxies for trace metal paleosources and paleocean circulation. *Geochimica et Cosmochimica Acta*, 63(10), 1489–1505. [https://doi.org/10.1016/s0016-7037\(99\)00068-x](https://doi.org/10.1016/s0016-7037(99)00068-x)
- Allredge, A. L., & Cohen, Y. (1987). Can microscale chemical patches persist in the sea? Microelectrode study of marine snow, fecal pellets. *Science*, 235(4789), 689–691. <https://doi.org/10.1126/science.235.4789.689>
- Allen, R. W., Collier, J. S., Stewart, A. G., Henstock, T., Goes, S., Rietbrock, A., et al. (2019). The role of arc migration in the development of the Lesser Antilles: A new tectonic model for the cenozoic evolution of the eastern Caribbean. *Geology*, 47(9), 891–895. <https://doi.org/10.1130/G46708.1>
- Ardelan, M. V., & Steinnes, E. (2010). Changes in mobility and solubility of the redox sensitive metals Fe, Mn and Co at the seawater-sediment interface following CO₂ seepage. *Biogeosciences*, 7(2), 569–583. <https://doi.org/10.5194/bg-7-569-2010>
- Barker, S., Greaves, M., & Elderfield, H. (2003). A study of cleaning procedures used for foraminiferal Mg/Ca paleothermometry. *Geochemistry, Geophysics, Geosystems*, 4(9), 1–20. <https://doi.org/10.1029/2003GC000559>
- Beaulieu, S. E., Baker, E. T., German, C. R., & Maffei, A. (2013). An authoritative global database for active submarine hydrothermal vent fields. *Geochemistry, Geophysics, Geosystems*, 14(11), 4892–4905. <https://doi.org/10.1002/2013GC004998>
- Bianchi, D., Weber, T. S., Kiko, R., & Deutsch, C. (2018). Global niche of marine anaerobic metabolisms expanded by particle microenvironments. *Nature Geoscience*, 11(4), 1–6. <https://doi.org/10.1038/s41561-018-0081-0>
- Bouysse, P., & Westercamp, D. (1990). Subduction of Atlantic aseismic ridges and late cenozoic evolution of the lesser Antilles Island Arc. *Tectonophysics*, 175(4), 349–380. [https://doi.org/10.1016/0040-1951\(90\)90180-G](https://doi.org/10.1016/0040-1951(90)90180-G)
- Boyle, E. A. (1983). Manganese carbonate overgrowths on foraminifera tests. *Geochimica et Cosmochimica Acta*, 47(10), 1815–1819. [https://doi.org/10.1016/0016-7037\(83\)90029-7](https://doi.org/10.1016/0016-7037(83)90029-7)
- Browning, T. J., Achterberg, E. P., Engel, A., & Mawji, E. (2021). Manganese co-limitation of phytoplankton growth and major nutrient draw-down in the Southern Ocean. *Nature Communications*, 12(1), 1–9. <https://doi.org/10.1038/s41467-021-21122-6>
- Burke, K. (1988). Tectonic evolution of the Caribbean. *Annual Review of Earth and Planetary Sciences*, 16(1), 201–230. <https://doi.org/10.1146/annurev.ea.16.050188.001221>
- Calais, É., Smithe, S., Mercier de Lépinay, B., & Prépetit, C. (2016). Plate boundary segmentation in the northeastern Caribbean from geodetic measurements and Neogene geological observations. *Comptes Rendus Geoscience*, 348(1), 42–51. <https://doi.org/10.1016/j.crte.2015.10.007>
- Calvert, S. E., & Pedersen, T. F. (1993). Geochemistry of recent and anoxic marine sediments: Implication for the geological records. *Marine Geology*, 113(1–2), 67–88. [https://doi.org/10.1016/0025-3227\(93\)90150-T](https://doi.org/10.1016/0025-3227(93)90150-T)
- Cassidy, M., Taylor, R. N., Palmer, M. R., Cooper, R. J., Stenlake, C., & Trofimovs, J. (2012). Tracking the magmatic evolution of island arc volcanism: Insights from a high-precision Pb isotope record of Montserrat, Lesser Antilles. *Geochemistry Geophysics Geosystems*, 13. <https://doi.org/10.1029/2012gc004064>
- Chatterjee, S. (1984). Variance estimation in factor analysis: An application of the bootstrap. *British Journal of Mathematical and Statistical Psychology*, 37(2), 252–262. <https://doi.org/10.1111/j.2044-8317.1984.tb00803.x>
- Chen, P., Yu, J., & Jin, Z. (2017). An evaluation of benthic foraminiferal U/Ca and U/Mn proxies for deep ocean carbonate chemistry and redox conditions. *Geochemistry, Geophysics, Geosystems*, 18(2), 617–630. <https://doi.org/10.1002/2016GC006730>

Acknowledgments

This research used samples provided by the Ocean Drilling Program (ODP). Reimund Jotter kindly supported the chemical analyses in the clean labs at the MPIC. The authors thank Antje Sorowka for her assistance in preparing samples for the NanoSIMS analysis. The authors are grateful to Elmar Gröner, Philipp Schuhmann, and Peter Hoppe for providing support at the NanoSIMS laboratory at the MPIC. Lead isotope data were obtained from the GeoROC database. Comments of anonymous reviewers helped us improve our manuscript. The authors are thankful to Adina Paytan for the editorial handling. Open access funding enabled and organized by Projekt DEAL.

- Cronan, D. S., & Johnson, A. (2001). Hydrothermal metalliferous sediments and waters off the Lesser Antilles. *Marine Georesources & Geotechnology*, 19(2), 65–83. <https://doi.org/10.1080/10641190109353805>
- Davis, C. V., Fehrenbacher, J. S., Benitez-Nelson, C., & Thunell, R. C. (2020). Trace element heterogeneity across individual Planktic foraminifera from the modern Cariaco basin. *Journal of Foraminiferal Research*, 50(2), 204–218. <https://doi.org/10.2113/gsjfr.50.2.204>
- De Schepper, S., Groeneveld, J., Naafs, B. D. A., Van Renterghem, C., Hennissen, J., Head, M. J., et al. (2013). Northern Hemisphere Glaciation during the globally warm early late Pliocene. *PLoS One*, 8(12), e81508. <https://doi.org/10.1371/journal.pone.0081508>
- Detlef, H., Sosdian, S. M., Kender, S., Lear, C. H., & Hall, I. R. (2020). Multi-elemental composition of authigenic carbonates in benthic foraminifera from the eastern Bering Sea continental margin (International Ocean Discovery Program Site U1343). *Geochimica et Cosmochimica Acta*, 268, 1–21. <https://doi.org/10.1016/j.gca.2019.09.025>
- Donnelly, T. W. (1973). Chapter 29: Circum-Caribbean explosive volcanic activity: Evidence from leg 15 sediments. In N. T. Edgar, A. G. Kaneps, & J. R. Herring (Eds.), *Initial reports of the Deep Sea Drilling Project* (Vol. 15, pp. 969–987). U.S.A.: University of California. <https://doi.org/10.2973/dsdp.proc.15.129.1973>
- Driscoll, N. W., & Diebold, J. B. (1999). Chapter 20 Tectonic and stratigraphic development of the eastern Caribbean: New constraints from multichannel seismic data. In P. Mann (Ed.), *Sedimentary basins of the world* (Vol. 4, pp. 591–626). Elsevier Special Publications. [https://doi.org/10.1016/S1874-5997\(99\)80054-9](https://doi.org/10.1016/S1874-5997(99)80054-9)
- Frank, M., Marbler, H., Koschinsky, A., Van De Fliedert, T., Klemm, V., Gutjahr, M., et al. (2006). Submarine hydrothermal venting related to volcanism in the Lesser Antilles: Evidence from ferromanganese precipitates. *Geochemistry, Geophysics, Geosystems*, 7(4). <https://doi.org/10.1029/2005GC001140>
- Friedrich, O., Wilson, P. A., Bolton, C. T., Beer, C. J., & Schiebel, R. (2013). Late Pliocene to early Pleistocene changes in the North Atlantic Current and suborbital-scale sea-surface temperature variability. *Paleoceanography*, 28(2), 274–282. <https://doi.org/10.1002/palo.20029>
- Fritz-Endres, T., & Fehrenbacher, J. (2020). Preferential loss of high trace element bearing inner calcite in foraminifera during physical and chemical cleaning. *Geochemistry, Geophysics, Geosystems*, 22(1). <https://doi.org/10.1029/2020GC009419>
- Froelich, P. N., Klinkhammer, G. P., Bender, M. L., Luedtke, N. A., Heath, G. R., Cullen, D., et al. (1979). Early oxidation of organic matter in pelagic sediments of the eastern equatorial Atlantic: Suboxic diagenesis. *Geochimica et Cosmochimica Acta*, 43(7), 1075–1090. [https://doi.org/10.1016/0016-7037\(79\)90095-4](https://doi.org/10.1016/0016-7037(79)90095-4)
- Gartman, A., & Findlay, A. J. (2020). Impacts of hydrothermal plume processes on oceanic metal cycles and transport. *Nature Geoscience*, 13(6), 396–402. <https://doi.org/10.1038/s41561-020-0579-0>
- Gooday, A. J., Turley, C. M., & Allen, J. A. (1990). Responses by benthic organisms to inputs of organic material to the ocean floor: A review. *Philosophical Transactions of the Royal Society of London - Series A: Mathematical and Physical Sciences*, 331(1616), 119–138. <https://doi.org/10.1098/rsta.1990.0060>
- Gröger, M., Henrich, R., & Bickert, T. (2003). Variability of silt grain size and planktonic foraminiferal preservation in Plio/Pleistocene sediments from the western equatorial Atlantic and Caribbean. *Marine Geology*, 201(4), 307–320. [https://doi.org/10.1016/S0025-3227\(03\)00264-0](https://doi.org/10.1016/S0025-3227(03)00264-0)
- Halbach, P., Marbler, H., Cronan, D. S., Koschinsky, A., Rahders, E., & Seifert, R. (2002). Submarine hydrothermal mineralisations and fluids off the Lesser Antilles Island arc – Initial results from the CARIBFLUX cruise SO 154. *InterRidge News*, 11(1), 18–22.
- Hammer, Ø., Harper, D. A. T., & Ryan, P. D. (2001). PAST: Paleontological statistics software package for education and data analysis. *Palaentologia Electronica*, 4(1), 1–9. <https://doi.org/10.1016/j.bcp.2008.05.025>
- Haug, G. H., & Tiedemann, R. (1998). Effect of the formation of the Isthmus of Panama on Atlantic Ocean thermohaline circulation. *Nature*, 393(6686), 673–676. <https://doi.org/10.1038/31447>
- Haug, G. H., Tiedemann, R., Zahn, R., & Ravelo, A. C. (2001). Role of Panama uplift on oceanic freshwater balance. *Geology*, 29(3), 207–210. [https://doi.org/10.1130/0091-7613\(2001\)029<0207:ROPUOO>2.0.CO;2](https://doi.org/10.1130/0091-7613(2001)029<0207:ROPUOO>2.0.CO;2)
- Homoky, W. B., Hembury, D. J., Hepburn, L. E., Mills, R. A., Statham, P. J., Fones, G. R., & Palmer, M. R. (2011). Iron and manganese diagenesis in deep sea volcanogenic sediments and the origins of pore water colloids. *Geochimica et Cosmochimica Acta*, 75(17), 5032–5048. <https://doi.org/10.1016/j.gca.2011.06.019>
- Hoppe, P., Cohen, S., & Meibom, A. (2013). NanoSIMS: Technical aspects and applications in cosmochemistry and biological geochemistry. *Geostandards and Geoanalytical Research*, 37(2), 111–154. <https://doi.org/10.1111/j.1751-908X.2013.00239.x>
- Jackson, T. A. (2013). A review of volcanic island evolution and magma production rate: An example from a Cenozoic Island arc in the Caribbean. *Journal of the Geological Society*, 170(3), 547–556. <https://doi.org/10.1144/jgs2011-166>
- Jain, S., Collins, L. S., & Hayek, L. A. C. (2007). Relationship of benthic foraminiferal diversity to paleoproductivity in the Neogene Caribbean. *Palaeoecology, Palaeclimatology, Palaeoecology*, 255(3–4), 223–245. <https://doi.org/10.1016/j.palaeo.2007.05.017>
- Jochum, K. P., Garbe-Schönberg, D., Veter, M., Stoll, B., Weis, U., Weber, M., et al. (2019). Nano-powdered calcium carbonate reference materials: Significant progress for microanalysis? *Geostandards and Geoanalytical Research*, 43(2), 1–15. <https://doi.org/10.1111/ggr.12292>
- Jochum, K. P., Stoll, B., Herwig, K., & Willbold, M. (2007). Validation of LA-ICP-MS trace element analysis of geological glasses using a new solid-state 193 nm Nd:YAG laser and matrix-matched calibration. *Journal of Analytical Atomic Spectrometry*, 22(2), 112–121. <https://doi.org/10.1039/b609547j>
- Johnson, J. E., Webb, S. M., Ma, C., & Fischer, W. W. (2016). Manganese mineralogy and diagenesis in the sedimentary rock record. *Geochimica et Cosmochimica Acta*, 173, 210–231. <https://doi.org/10.1016/j.gca.2015.10.027>
- Jorissen, F. J., Fontanier, C., & Thomas, E. (2007). Paleoclimatological proxies based on deep-sea benthic foraminiferal assemblage characteristics. In C. Hillaire-Marcel & A. de Vernal (Eds.), *Developments in marine geology: Proxies in Late Cenozoic Paleoclimatology* (Vol. 1, pp. 263–325). [https://doi.org/10.1016/S1572-5480\(07\)01012-3](https://doi.org/10.1016/S1572-5480(07)01012-3)
- Kirillova, V., Osborne, A. H., Störöling, T., & Frank, M. (2019). Miocene restriction of the Pacific-North Atlantic throughflow strengthened Atlantic overturning circulation. *Nature Communications*, 10(1), 4025. <https://doi.org/10.1038/s41467-019-12034-7>
- Klinkhammer, G. P., Mix, A. C., & Haley, B. A. (2009). Increased dissolved terrestrial input to the coastal ocean during the last deglaciation. *Geochemistry, Geophysics, Geosystems*, 10(3). <https://doi.org/10.1029/2008GC002219>
- Koschinsky, A., Seifert, R., Knappe, A., Schmidt, K., & Halbach, P. (2007). Hydrothermal fluid emanations from the submarine Kick'em Jenny volcano, Lesser Antilles island arc. *Marine Geology*, 244(1–4), 129–141. <https://doi.org/10.1016/j.margeo.2007.06.013>
- Kozdon, R., Kelly, D. C., Kitajima, K., Strickland, A., Fournelle, J. H., & Valley, J. W. (2013). In situ $\delta^{18}\text{O}$ and Mg/Ca analyses of diagenetic and planktic foraminiferal calcite preserved in a deep-sea record of the Paleocene-Eocene thermal maximum. *Paleoceanography*, 28(3), 517–528. <https://doi.org/10.1002/palo.20048>
- Kumar, A., Abouchami, W., Galer, S. J. G., Singh, S. P., Fomba, K. W., Prospero, J. M., & Andreae, M. O. (2018). Seasonal radiogenic isotopic variability of the African dust outflow to the tropical Atlantic Ocean and across to the Caribbean. *Earth and Planetary Science Letters*, 487, 94–105. <https://doi.org/10.1016/j.epsl.2018.01.025>

- Labanieh, S., Chauvel, C., Germa, A., Quidelleur, X., & Lewin, E. (2010). Isotopic hyperbolas constrain sources and processes under the Lesser Antilles arc. *Earth and Planetary Science Letters*, 298(1–2), 35–46. <https://doi.org/10.1016/j.epsl.2010.07.018>
- Lear, C. H., Elderfield, H., & Wilson, P. A. (2000). Cenozoic deep-sea temperatures and global ice volumes from Mg/Ca in benthic foraminiferal calcite. *Science*, 287(5451), 269–272. <https://doi.org/10.1126/science.287.5451.269>
- Lemelle, L., Bartolini, A., Simionovici, A., Tucoulou, R., De Nolf, W., Bassinot, F., & de Garidel-Thoron, T. (2020). Nanoscale trace metal imprinting of biocalcification of planktic foraminifers by Toba's super-eruption. *Scientific Reports*, 10(1), 1–12. <https://doi.org/10.1038/s41598-020-67481-w>
- Lindsay, J. M., Trumbull, R. B., & Siebel, W. (2005). Geochemistry and petrogenesis of late Pleistocene to Recent volcanism in Southern Dominica, Lesser Antilles. *Journal of Volcanology and Geothermal Research*, 148(3–4), 253–294. <https://doi.org/10.1016/j.jvolgeores.2005.04.018>
- Luther, G. W., III., Sundby, B., Lewis, B. L., Brendel, P. J., & Silverberg, N. (1997). Interactions of manganese with the nitrogen cycle: Alternative pathways to dinitrogen. *Geochimica et Cosmochimica Acta*, 61(19), 4043–4052. [https://doi.org/10.1016/S0016-7037\(97\)00239-1](https://doi.org/10.1016/S0016-7037(97)00239-1)
- Martin, J. H., & Knauer, G. A. (1980). Manganese cycling in northeast Pacific waters. *Earth and Planetary Science Letters*, 51(2), 266–274. [https://doi.org/10.1016/0012-821X\(80\)90209-5](https://doi.org/10.1016/0012-821X(80)90209-5)
- McGee, L., Reagan, M., Turner, S., Sparks, R. S., Handley, H., Didonna, R., et al. (2021). U-series histories of magmatic volatile phase and enclave development at Soufrière Hills Volcano, Montserrat. *Chemical Geology*, 559, 119957. <https://doi.org/10.1016/j.chemgeo.2020.119957>
- Middag, R., de Baar, H. J. W., Laan, P., & Klunder, M. B. (2011). Fluvial and hydrothermal input of manganese into the Arctic Ocean. *Geochimica et Cosmochimica Acta*, 75(9), 2393–2408. <https://doi.org/10.1016/j.gca.2011.02.011>
- Middag, R., de Baar, H. J. W., Laan, P., Cai, P. H., & van Ooijen, J. C. (2011). Dissolved manganese in the Atlantic sector of the southern ocean. *Deep-Sea Research Part II Topical Studies in Oceanography*, 58(25–26), 2661–2677. <https://doi.org/10.1016/j.dsr2.2010.10.043>
- Munsel, D., Kramar, U., Dissard, D., Nehrke, G., Berner, Z., Bijma, J., et al. (2010). Heavy metal incorporation in foraminiferal calcite: Results from multi-element enrichment culture experiments with *Ammonia tepida*. *Biogeosciences*, 7(8), 2339–2350. <https://doi.org/10.5194/bg-7-2339-2010>
- Münch, P. H., Cornee, J. J., Lebrun, J. F., Quillevère, F., Verati, C., Melinte-Dobrincescu, M., et al. (2014). Pliocene to pleistocene vertical movements in the forearc of the Lesser Antilles subduction: Insights from chronostratigraphy of shallow-water carbonate platforms (Guadeloupe archipelago). *Journal of the Geological Society*, 171(3), 329–341. <https://doi.org/10.1144/jgs2013-005>
- Newkirk, D. R., & Martin, E. E. (2009). Circulation through the Central American Seaway during the Miocene carbonate crash. *Geology*, 37(1), 87–90. <https://doi.org/10.1130/G25193A.1>
- Ni, S., Quintana Krupinski, N. B., Groeneveld, J., Persson, P., Somogyi, A., Brinkmann, I., et al. (2020). Early diagenesis of foraminiferal calcite under anoxic conditions: A case study from the Landsort Deep, Baltic Sea (IODP site M0063). *Chemical Geology*, 558, 119871. <https://doi.org/10.1016/j.chemgeo.2020.119871>
- Ni Fhlaithearta, S., Fontanier, C., Jorissen, F., Mouret, A., Dueñas-Bohórquez, A., Anschutz, P., et al. (2018). Manganese incorporation in living (stained) benthic foraminiferal shells: A bathymetric and in-sediment study in the Gulf of Lions (NW Mediterranean). *Biogeosciences*, 15(20), 6315–6328. <https://doi.org/10.5194/bg-15-6315-2018>
- Nürnberg, D., Bijma, J., & Hemleben, C. (1996). Assessing the reliability of magnesium in foraminiferal calcite as a proxy for water mass temperatures. *Geochimica et Cosmochimica Acta*, 60(5), 803–814. [https://doi.org/10.1016/0016-7037\(95\)00446-7](https://doi.org/10.1016/0016-7037(95)00446-7)
- Osborne, A. H., Newkirk, D. R., Groeneveld, J., Martin, E. E., Tiedemann, R., & Frank, M. (2014). The seawater neodymium and lead isotope record of the final stages of Central American Seaway closure. *Paleoceanography*, 29(7), 715–729. <https://doi.org/10.1002/2014PA002676>
- O'Dea, A., Lessios, H. A., Coates, A. G., Eytan, R. I., Restrepo-Moreno, S. A., Cione, A. L., et al. (2016). Formation of the Isthmus of Panama. *Science Advances*, 2(8), 1–11. <https://doi.org/10.1126/sciadv.1600883>
- Ögretmen, N., Schiebel, R., Jochum, K. P., Stoll, B., Weis, U., Repschläger, J., et al. (2020a). Analyses on *Cibicides* wuellerstorfi from ODP Hole 165-999A [Dataset], PANGAEA - Data Publisher for Earth and Environmental Science. <https://doi.org/10.1594/PANGAEA.921108>
- Ögretmen, N., Schiebel, R., Jochum, K. P., Stoll, B., Weis, U., Repschläger, J., et al. (2020b). Deep Thermohaline Circulation Across the Closure of the Central American Seaway. *Paleoceanography and Paleoclimatology*, 35(12). <https://doi.org/10.1029/2020pa004049>
- Pearson, P. N., & Burgess, C. E. (2008). Foraminifer test preservation and diagenesis: comparison of high latitude Eocene sites. *Geological Society, London, Special Publications*, 303(1), 59–72. <https://doi.org/10.1144/sp303.5>
- Pingitore, N. E. (1978). The behavior of Zn²⁺ and Mn²⁺ during carbonate diagenesis; theory and applications. *Journal of Sedimentary Research*, 48(3), 799–814.
- Poirier, R. K., Gaetano, M. Q., Acevedo, K., Schaller, M. F., Raymo, M. E., & Kozdon, R. (2021). Quantifying diagenesis, contributing factors, and resulting isotopic bias in benthic foraminifera using the foraminiferal preservation index: Implications for geochemical proxy records. *Paleoceanography and Paleoclimatology*, 36(5). e2020PA004110. <https://doi.org/10.1029/2020PA004110>
- Rathburn, A. E., & Corliss, B. H. (1994). The ecology of living (stained) deep-sea benthic foraminifera from the Sulu Sea. *Paleoceanography*, 9(1), 87–150. <https://doi.org/10.1029/93PA02327>
- Reichart, G. J., Jorissen, F., Anschutz, P., & Mason, P. R. D. (2003). Single foraminiferal test chemistry records the marine environment. *Geology*, 31(4), 355–358. [https://doi.org/10.1130/0091-7613\(2003\)031<0355:SFTCRT>2.0.CO;2](https://doi.org/10.1130/0091-7613(2003)031<0355:SFTCRT>2.0.CO;2)
- Resing, J. A., Sedwick, P. N., German, C. R., Jenkins, W. J., Moffett, J. W., Sohst, B. M., & Tagliabue, A. (2015). Basin-scale transport of hydrothermal dissolved metals across the South Pacific Ocean. *Nature*, 523(7559), 200–203. <https://doi.org/10.1038/nature14577>
- Robertson, R. E. A. (2009). Antilles, Geology. In R. G. Gillespie & D. A. Clague (Eds.), *Encyclopedia of Islands* (pp. 29–35). University of California Press. <https://doi.org/10.1525/9780520943728-010>
- Sayani, H. R., Thompson, D. M., Carilli, J. E., Marchitto, T. M., Chapman, A. U., & Cobb, K. M. (2021). Reproducibility of coral Mn/Ca-based wind reconstructions at Kiritimati Island and Butaritari Atoll. *Geochemistry, Geophysics, Geosystems*, 22(3). e2020GC009398. <https://doi.org/10.1029/2020gc009398>
- Schenau, S. J., Reichart, G. J., & De Lange, G. J. (2004). Oxygen minimum zone controlled Mn redistribution in Arabian Sea sediments during the Late Quaternary. *Paleoceanography*, 15(4), 1058. <https://doi.org/10.1029/2000PA000621>
- Schlitzer, R., Anderson, R. F., Dodas, E. M., Lohan, M., Geibert, W., Tagliabue, A., et al. (2018). The GEOTRACES intermediate data Product 2017. *Chemical Geology*, 493, 210–223. <https://doi.org/10.1016/j.chemgeo.2018.05.040>
- Schmuker, B., & Schiebel, R. (2002). Planktic foraminifers and hydrography of the eastern and northern Caribbean Sea. *Marine Micropaleontology*, 46(3–4), 387–403. [https://doi.org/10.1016/S0377-8398\(02\)00082-8](https://doi.org/10.1016/S0377-8398(02)00082-8)
- Schneider, A., Crémère, A., Panieri, G., Lepland, A., & Knies, J. (2017). Diagenetic alteration of benthic foraminifera from a methane seep site on Vestnesa Ridge (NW Svalbard). *Deep-Sea Research Part I Oceanographic Research Papers*, 123, 22–34. <https://doi.org/10.1016/j.dsr.2017.03.001>
- Schoemann, V., De Baar, H. J. W., De Jong, J. T. M., & Lancelot, C. (1998). Effects of phytoplankton blooms on the cycling of manganese and iron in coastal waters. *Limnology & Oceanography*, 43(7), 1427–1441. <https://doi.org/10.4319/lo.1998.43.7.1427>

- Schöne, B. R., Huang, X., Zettler, M. L., Zhao, L., Mertz-Kraus, R., Jochum, K. P., & Walliser, E. O. (2021). Mn/Ca in shells of Arctic islandica (Baltic Sea) – a potential proxy for ocean hypoxia? *Estuarine, Coastal and Shelf Science*, 251, 107257. <https://doi.org/10.1016/j.eess.2021.107257>
- Seki, O., Foster, G. L., Schmidt, D. N., Mackensen, A., Kawamura, K., & Pancost, R. D. (2010). Alkenone and boron-based Pliocene pCO₂ records. *Earth and Planetary Science Letters*, 292(1–2), 201–211. <https://doi.org/10.1016/j.epsl.2010.01.037>
- Sexton, P. F., Wilson, P. A., & Pearson, P. N. (2006). Microstructural and geochemical perspectives on planktic foraminiferal preservation: “glassy” versus “frosty”. *Geochemistry, Geophysics, Geosystems*, 7(12). <https://doi.org/10.1029/2006GC001291>
- Shanks, A. L., & Reeder, M. L. (1993). Reducing microzones and sulfide production in marine snow. *Marine Ecology Progress Series*, 96(1), 43–47. <https://doi.org/10.3354/meps096043>
- Shepherd, J. G., Brewer, P. G., Oschlies, A., & Watson, A. J. (2017). Ocean ventilation and deoxygenation in a warming world: Introduction and overview. *Philosophical Transactions of the Royal Society A: Mathematical, Physical & Engineering Sciences*, 375(2102), 20170240. <https://doi.org/10.1098/rsta.2017.0240>
- Shipboard Scientific Party. (1997). Caribbean volcanism, cretaceous/tertiary impact, and ocean-climate history: Synthesis of leg 165. In H. Sigurdsson, R. M. Leckie, & G. D. Acton (Eds.), *Proceedings of the ocean drilling program, 165 initial reports* (Vol. 165, pp. 377–400). <https://doi.org/10.2973/odp.proc.ir.165.108.1997>
- Sigurdsson, H., Leckie, R., & Acton, G. D. (1997). Site 999, initial reports. *Proceedings of the Ocean Drilling Program*, (Vol. 165, 131–230).
- Soldati, A. L., Jacob, D. E., Glatzel, P., Swarbrick, J. C., & Geck, J. (2016). Element substitution by living organisms: The case of manganese in mollusc shell aragonite. *Scientific Reports*, 6, 1–9. <https://doi.org/10.1038/srep22514>
- Son, S., Newton, A. G., Jo, K., Lee, J. Y., & Kwon, K. D. (2019). Manganese speciation in Mn-rich CaCO₃: A density functional theory study. *Geochimica et Cosmochimica Acta*, 248, 231–241. <https://doi.org/10.1016/j.gca.2019.01.011>
- Steph, S., Tiedemann, R., Prange, M., Groeneveld, J., Nürnberg, D., Reuning, L., et al. (2006). Changes in Caribbean surface hydrography during the Pliocene shoaling of the Central American Seaway. *Paleoceanography*, 21(4), 1–25. <https://doi.org/10.1029/2004PA001092>
- Steph, S., Tiedemann, R., Prange, M., Groeneveld, J., Schulz, M., Timmermann, A., et al. (2010). Early Pliocene increase in thermohaline overturning: A precondition for the development of the modern equatorial Pacific cold tongue. *Paleoceanography*, 25(2). <https://doi.org/10.1029/2008PA001645>
- Sturges, W. (1970). Observations of deep-water renewal in the Caribbean Sea. *Journal of Geophysical Research*, 75(36), 7602–7610. <https://doi.org/10.1029/jc075i036p07602>
- Sunda, W. G., Huntsman, S. A., & Harvey, G. R. (1983). Photoreduction of manganese oxides in seawater and its geochemical and biological implications. *Nature*, 301(5897), 234–236. <https://doi.org/10.1038/301234a0>
- Thirlwall, M. F., Graham, A. M., Arculus, R. J., Harmon, R. S., & Macpherson, C. G. (1996). Resolution of the effects of crustal assimilation, sediment subduction, and fluid transport in island arc magmas: PbSrNdO isotope geochemistry of Grenada, Lesser Antilles. *Geochimica et Cosmochimica Acta*, 60(23), 4785–4810. [https://doi.org/10.1016/s0016-7037\(96\)00272-4](https://doi.org/10.1016/s0016-7037(96)00272-4)
- Thomas, E., & Gooday, A. J. (1996). Cenozoic deep-sea benthic foraminifers: Tracers for changes in oceanic productivity? *Geology*, 24(4), 355–358. [https://doi.org/10.1130/0091-7613\(1996\)024<0355:CDSBFT>2.3.CO;2](https://doi.org/10.1130/0091-7613(1996)024<0355:CDSBFT>2.3.CO;2)
- Thompson, D. M., Cole, J. E., Shen, G. T., Tudhope, A. W., & Meehl, G. A. (2015). Early twentieth-century warming linked to tropical Pacific wind strength. *Nature Geoscience*, 8(2), 117–121. <https://doi.org/10.1038/ngeo2321>
- Torres, M. E., Martin, R. A., Klinkhammer, G. P., & Nesbitt, E. A. (2010). Post depositional alteration of foraminiferal shells in cold seep settings: New insights from flow-through time-resolved analyses of biogenic and inorganic seep carbonates. *Earth and Planetary Science Letters*, 299(1–2), 10–22. <https://doi.org/10.1016/j.epsl.2010.07.048>
- Trouwborst, R. E., Clement, B. G., Tebo, B. M., Glazer, B. T., & Luther, G. W. (2006). Soluble Mn(III) in suboxic zones. *Science*, 313(5795), 1955–1957. <https://doi.org/10.1126/science.1132876>
- van Hulst, M., Middag, R., Dutay, J. C., De Baar, H., Roy-Barman, M., Gehlen, M., et al. (2017). Manganese in the west Atlantic Ocean in the context of the first global ocean circulation model of manganese. *Biogeosciences*, 14(5), 1123–1152. <https://doi.org/10.5194/bg-14-1123-2017>
- von Blanckenburg, F., O’Nions, R. K., & Heinz, J. R. (1996). Distribution and sources of pre-anthropogenic lead isotopes in deep ocean water from FeMn crusts. *Geochimica et Cosmochimica Acta*, 60(24), 4957–4963. [https://doi.org/10.1016/s0016-7037\(96\)00310-9](https://doi.org/10.1016/s0016-7037(96)00310-9)
- Webber, A. P., Roberts, S., Murton, B. J., & Hodgkinson, M. R. S. (2014). Geology, sulfide geochemistry and supercritical venting at the Beebe Hydrothermal Vent Field, Cayman Trough. *Geochemistry, Geophysics, Geosystems*, 16(8), 2661–2678. <https://doi.org/10.1002/2015GC005879>
- Wegner, W., Wörner, G., Harmon, R. S., & Jicha, B. R. (2011). Magmatic history and evolution of the central American land bridge in Panama since Cretaceous times. *Bulletin of the Geological Society of America*, 123(3–4), 703–724. <https://doi.org/10.1130/B30109.1>
- Wong, K. H., Nishioka, J., Kim, T., & Obata, H. (2022). Long-range lateral transport of dissolved manganese and iron in the subarctic Pacific. *Journal of Geophysical Research: Oceans*, 127(2). e2021JC017652. <https://doi.org/10.1029/2021jc017652>
- Wu, M., McCain, J. S. P., Rowland, E., Middag, R., Sandgren, M., Allen, A. E., & Bertrand, E. M. (2019). Manganese and iron deficiency in Southern Ocean Phaeocystis Antarctica populations revealed through taxon-specific protein indicators. *Nature Communications*, 10(1), 1–10. <https://doi.org/10.1038/s41467-019-11426-z>
- Yu, J., Elderfield, H., & Hönisch, B. (2007). B/Ca in planktonic foraminifera as a proxy for surface seawater pH. *Paleoceanography*, 22(2). <https://doi.org/10.1029/2006PA001347>
- Yücel, M., Sevgen, S., & Le Bris, N. (2021). Soluble, Colloidal, and Particulate Iron Across the Hydrothermal Vent Mixing Zones in Broken Spur and Rainbow, Mid-Atlantic Ridge. *Frontiers in Microbiology*, 12. <https://doi.org/10.3389/fmicb.2021.631885>

References From the Supporting Information

- Garcia, H. E., Boyer, T. P., Locarnini, R. A., Antonov, J. I., Mishonov, A. V., Baranova, O. K., et al. (2013). World ocean atlas 2013. Volume 3: Dissolved oxygen, apparent oxygen utilization, and oxygen saturation. *NOAA Atlas NESDIS*, 75(3), 27.
- Garcia, H. E., Locarnini, R., Boyer, T. P., Antonov, J. I., Baranova, O. K., Zweng, M. M., et al. (2013). World ocean atlas 2013 volume 4: Nutrients (phosphate, nitrate, silicate). *NOAA Atlas NESDIS*, 76(4), 396.
- Jochum, K. P., Stoll, B., Weis, U., Jacob, D. E., Mertz-Kraus, R., & Andreae, M. O. (2014). Non-matrix-matched calibration for the multi-element analysis of geological and environmental samples using 200 nm femtosecond LA-ICP-MS: A comparison with nanosecond lasers. *Geostandards and Geoanalytical Research*, 38(3), 265–292. <https://doi.org/10.1111/j.1751-908X.2014.12028.x>
- Schlitzer, R. (2018). Ocean data view. Retrieved from <https://odv.awi.de/>